Available online at www.sciencedirect.com
ScienceDirect
Ceramics International 36 (2010) 1911–1916
CERAMICS INTERNATIONAL
www.elsevier.com/locate/ceramint

Influence of the sintering temperature on the structural feature and bioactivity of sol–gel derived SiO_2–CaO–P_2O_5 bioglass

J. Ma [a,b], C.Z. Chen [a,b,*], D.G. Wang [a,b], X.G. Meng [a,b], J.Z. Shi [a,b]

[a] Key Laboratory for Liquid-Solid Structural Evolution & Processing of Materials, Ministry of Education, Shandong University, Shandong 250061, China
[b] School of Materials Science and Engineering, Shandong University, Shandong 250061, China

Received 16 December 2009; received in revised form 10 January 2010; accepted 20 March 2010
Available online 28 April 2010

Abstract

A sol–gel method was utilized to synthesize the gel with the composition of 58 mol% SiO_2–38 mol% CaO–4 mol% P_2O_5. The thermal properties were studied using thermogravimetric and differential thermal analysis (TG/DTA). Then the gels were sintered at 700, 900, 1000 and 1200 °C. The structure features were characterized by X-ray diffraction (XRD), Fourier transform infrared spectroscopy (FTIR) and scanning electron microscopy (SEM), in addition in vitro assays were carried out in simulated body fluid (SBF). The results revealed that at sintering temperature above 900 °C, crystallization occurred and glass-ceramics with pseudowollastonite and wollastonite were formed. Furthermore with the increase of sintering temperature, the amount of pseudowollastonite decreased while that of wollastonite increased. In vitro tests indicated that the crystallization did not inhibit the samples bioactivity. After soaking in SBF, the formation of apatite was confirmed on glass and glass-ceramics surface, and the bioactivity of the glass-ceramics was based on the formed pseudowollastonite and wollastonite.

Keywords: A. Sol–gel; D. Glass; D. Glass-ceramics; E. Biomedical applications

1. Introduction

Since the discovery of the first bioactive glasses by Hench et al. [1], a new concept of bioactivity has been proposed and opened a novel research area on bioactive materials for bone repair and substitution [2–5]. A common character of these bioactive materials is identified as their capability for bone bonding, which is attributed to the formation of an apatite layer on their surface with composition and structure equivalent to the mineral phase of bone [6]. At present, a few methods have been utilized to prepare the bioactive glasses. Melting method, as a traditional way for glasses preparation, is simple and suitable for massive production [7,8]. However, during the high-temperature operation, the volatile components such as Na_2O, P_2O_5, etc. tend to escape from initial composition, and it is found that the limit of SiO_2 content for bioactivity was about 60 mol% [9]. On the other hand, the sol–gel technique, as a chemical method, attracts more researchers' interest and provides an available way to synthesize bioactive glasses. Compared with the traditional melting method, the sol–gel technique has the advantage of lower reaction temperature and allows us to obtain glasses with higher purity and homogeneity [10]. More importantly, glasses derived by sol–gel technique allow the expansion of bioactive compositional range up to 90 mol% SiO_2 [11].

However, the mechanical strength of these bioactive glasses is insufficient. Most of them have a less flexural strength and fracture toughness than those of human bone and possess greater elastic modulus. It means that most bioactive glasses have a less optimal mechanical compatibility when they are used in load-bearing applications. In 1982, Kokubo et al. [12] developed A/W glass-ceramics in the SiO_2–CaO–MgO–P_2O_5–CaF_2 system. After crystallization, the obtained glass-ceramics approximately contains 38 wt.% apatite and 24 wt.% wollastonite, and researches shows that this composite material can bond to living bone in a short time and possesses high mechanical strength for a long period in vivo [13–15]. Obviously, glass-ceramics, one kind of polycrystalline materials formed by controlling the crystallization from initial glasses, provides great possibilities to

* Corresponding author at: Key Laboratory for Liquid-Solid Structural Evolution & Processing of Materials, Ministry of Education, Shandong University, Shandong 250061, China. Tel.: +86 531 88395991;
fax: +86 531 88395991.
E-mail address: czchen@sdu.edu.cn (C.Z. Chen).

0272-8842/$36.00
doi:10.1016/j.ceramint.2010.03.017

optimize their properties, through the control of the composition, extent of crystallization, crystal morphology and crystal size.

The aim of this work was to obtain bioactive sol–gel glass-ceramics with the simplest composition and to study the influence of the crystallization induced in the sintering process on the structural features and bioactive properties. Therefore, the ternary system SiO_2–CaO–P_2O_5 was selected and the chosen sample was the 58S sol–gel derived bioglass. Fourier transform infrared spectroscopy (FTIR), X-ray diffraction (XRD) and scanning electron microscopy (SEM) were used to characterize the crystallization and structure changes and it was expected to investigate the influence of these variables on the bioactivity of obtained materials.

2. Experimental

2.1. Synthesis

Sol–gel derived 58S bioglass with the composition of 58 mol% SiO_2–38 mol% CaO–4 mol% P_2O_5 was synthesized in the study. The sample was prepared by hydrolysis and polycondensation of tetraethyl orthosilicate (TEOS), triethyl phosphate (TEP), and $Ca(NO_3)_2{\cdot}4H_2O$. Nitric acid (2N) was used to as catalyst with a molar ratio of HNO_3/(TEOS + TEP) = 0.05. Each reactant was consecutively added under continuous stirring. Then the sol was introduced into polyethylene containers at room temperature till the gel appeared. For aging, the gel was kept at 60 °C for 3 days and then the drying process was carried out at 120 °C, followed by 4 h ball milling to obtain the powders with sizes ranging from 38 to 74 μm. Finally, the gel powders were respectively sintered at 700, 900, 1000 and 1200 °C for 3 h with a heating rate of 5 °C/min, then the furnace was naturally cooled down.

2.2. Characterization

The thermogravimetric and differential thermal analysis (TG/DTA) were carried out on SDT Q600 of TA Instruments with a 5 °C/min heating rate under an air atmosphere. The crystallization of the samples was examined in a Bruker D8 Advance X-ray diffractometer using CuK_a radiation (λ = 1.5406 nm) produced at 40 kV and 40 mA and the range of diffraction angles (2θ) was scanned between 10° and 70° with a step size of 0.02°/s. FTIR analysis was conducted in a Bruker Optics VERTEX-70 spectrometer using the KBr pellets technique. Microstructure of samples was observed in a JEOL-JSM 6380LA scanning electron microscope.

In vitro tests were performed by soaking the samples in simulated body fluid (SBF), which contains an ionic composition similar to that of human plasma [16], at 37 °C in sterile polyethylene containers. During immersion, a constant solid mass/liquid volume (0.1 g/100 ml) ratio was maintained and the SBF solution was replaced every 2 days. After being soaked, samples were rinsed with deionized water and acetone and then dried in air at room temperature. The formation of an apatite-like layer on the samples surface was determined by XRD, SEM, and FTIR analysis as described above.

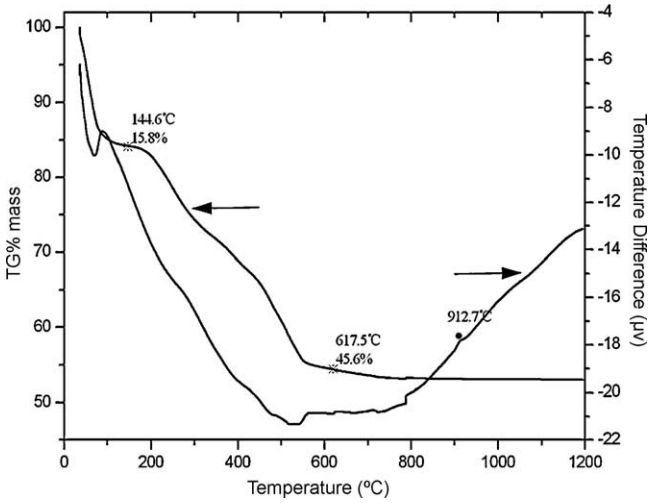

Fig. 1. TG and DTA curves of the gel powders after being dried at 120 °C.

3. Results

3.1. Thermal property analysis

Fig. 1 shows the TG/DTA curves of the gel dried at 120 °C. From the TG curve, it is observed that two obvious weight losses occur. An initial process in the range of room temperature to 144.6 °C is attributed to the loss of residual water and ethanol, corresponding to a weight loss of 15.8%. Then the second process occurs at 617.5 °C with a weight loss of 45.6%. Finally, the weight remains constant up to 1200 °C. In addition, an exothermic peak in the range of 890–926 °C is detected on the DTA curve, where the peak crystallization temperature (T_p) is 912.7 °C.

3.2. Crystallization analysis

The crystallization of the sample sintered at various temperatures is shown in Fig. 2. It can be seen that amorphous powders were obtained when the gels were sintered at 700 °C. With further increase of the temperature, sharp peaks appeared,

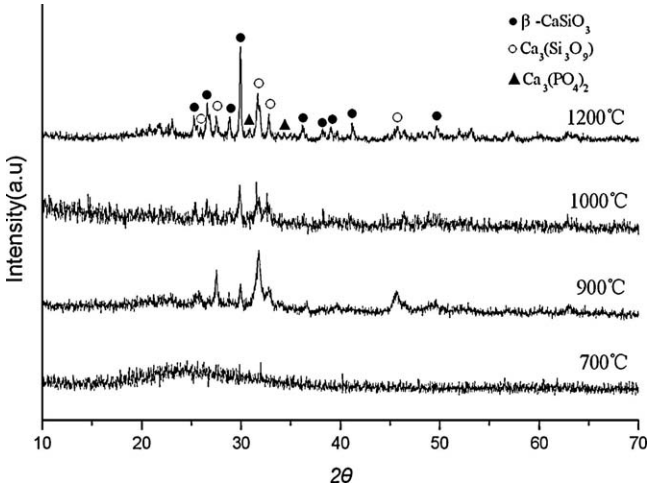

Fig. 2. XRD patterns of the sample sintered at various temperatures.

indicating the crystallization. After sintering at 900 °C, the sample pattern was agreement with the standard XRD patterns for pseudowollastonite $Ca_3(Si_3O_9)$ (JCPDS 74-0874) and wollastonite β-$CaSiO_3$ (JCPDS 42-0547). $Ca_3(Si_3O_9)$ was the principal phase and it is notable that the formation temperature of high-temperature phase $Ca_3(Si_3O_9)$ was clearly decreased. However, after being sintered at 1000 and 1200 °C, the amount of $Ca_3(Si_3O_9)$ phase decreased with simultaneous increase of β-$CaSiO_3$. In addition, a little diffraction peaks assigned to tricalcium phosphate $Ca_3(PO_4)_2$ (JCPDS 09-0169) were also detected.

Fig. 3 shows the FTIR spectra of samples sintered at various temperatures. The FTIR spectra of samples sintered at 700 °C showed the characteristic bands for sol–gel glasses. According to the previous literatures [17–20], three optical vibration modes of Si–O group are observed. The band at 1090 cm^{-1} corresponds to the asymmetric stretching mode Si–O–Si (s, asym), the one at 800 cm^{-1} is associated to symmetric stretching vibration Si–O–Si (s, sym) and the one at around 460 cm^{-1} is identified as rocking vibration Si–O–Si (r). In addition, the shoulder at 950 cm^{-1} is related to the non-bridging oxygen bonds (NBO) of Si–O–Ca. Besides the above

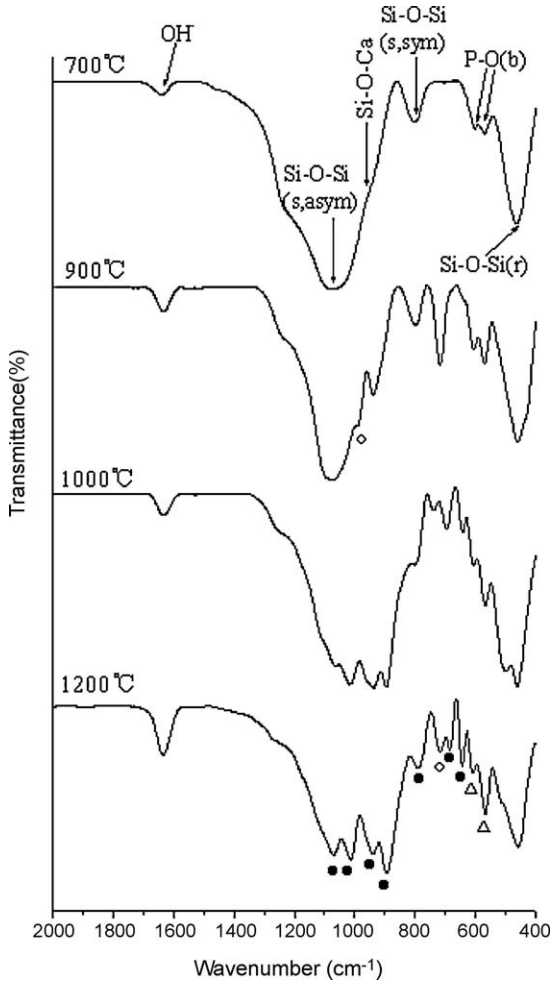

Fig. 3. FTIR spectra of samples sintered at different temperatures. Symbols are related to the vibration modes of pseudowollastonite (○), wollastonite (●) and tricalcium phosphate (△).

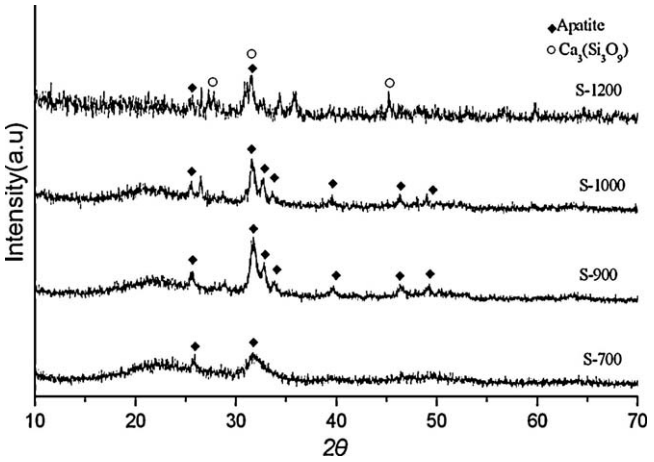

Fig. 4. XRD patterns of samples sintered at different temperatures after 7 days of soaking in SBF.

bands, the peaks at 570 and 603 cm^{-1} are assigned to the bending vibration P–O (b) corresponding to the crystalline phosphates and the vibration around 1630 cm^{-1} due to the deformation mode of H–O–H is also observed. After being sintered at 900 °C, new vibration bands appeared at 988, 936 and 718 cm^{-1}. And when the sintering temperature was over 900 °C, the spectra of samples sintered at 1000 and 1200 °C were similar and showed new characteristic, where the remarkable band at 718 cm^{-1} relating to pseudowollastonite decreased with temperature increasing. Furthermore, two bands at 606 and 568 cm^{-1} corresponding to the tricalcium phosphate (TCP) were also observed.

3.3. In vitro assays

Fig. 4 shows the XRD patterns of samples after 7 days of soaking in SBF, the characteristic peaks of apatite (JCPDS 24-0033) are obviously found. Compared with the amorphous structure before immersion, after 7 days of soaking the XRD pattern of sample sintered at 700 °C showed two wide diffraction peaks corresponding to (0 0 2) and (2 1 1) reflections of an apatite phase. As mentioned above, at higher temperatures (900–1200 °C), crystallization occurred and glass-ceramics were formed. However, crystallization did not inhibit the samples bioactivity. When the glass-ceramics were soaked in SBF for 7 days, the apatite was also detected. In addition, the reflections corresponding to the wollastonite existing in the glass-ceramics were not observed, even for the samples heated at 1200 °C where wollastonite was the majority phase. These results indicate the dissolution of wollastonite during the soaking which agreed with the works previously reported [21,22].

The surface modifications of samples sintered at various temperatures after soaking in SBF for 7 days were measured by FTIR and the results are given in Fig. 5. After 7 days of soaking, phosphate absorption bands at 1043, 603, 568 and 469 cm^{-1} were observed in all samples, where the doublet peaks at 603 and 568 cm^{-1} are characteristic feature of phosphate in crystalline phases [23,24]. Besides the bands above mentioned,

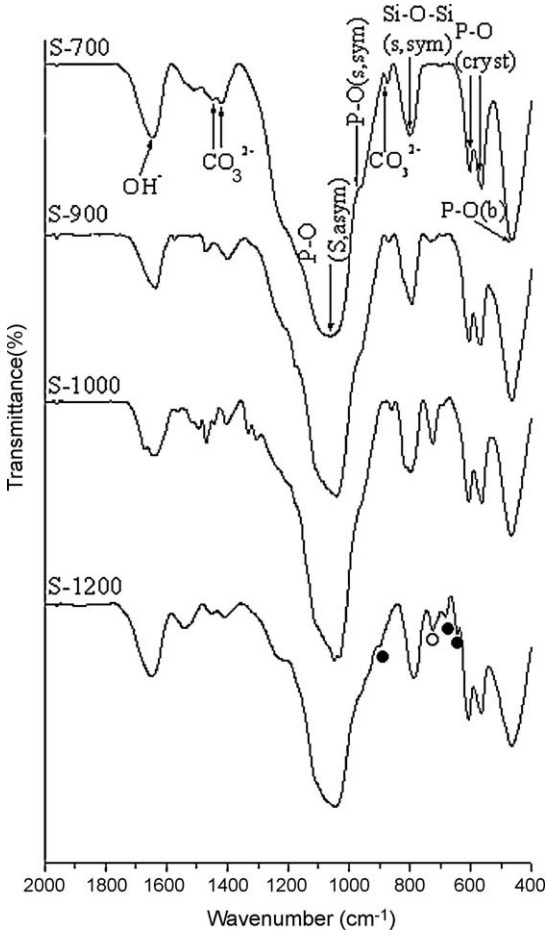

Fig. 5. FTIR spectra of samples sintered at different temperatures after 7 days of soaking in SBF. Symbols are related to the vibration modes of pseudowollastonite (○) and wollastonite (●).

carbonate adsorption bands at 1490, 1423 and 874 cm^{-1} were also detected. The appearance of the phosphate and carbonate absorption bands did not only confirm the formation of an apatite-like layer but also determine that the newly formed layer was a carbonate hydroxyapatite. Moreover, for the samples sintered at 900, 1000 and 1200 °C, the intensity of the bonds corresponding to pseudowollastonite and wollastonite decreased when they were soaked in SBF for 7 days. According to previous literatures [25,26], the dissolution studies show that those two phases are degradable and they are bioactive confirmed by the formation of apatite layer on their surfaces after soaking in SBF. Therefore, the intensity decrease of pseudowollastonite and wollastonite after soaking in SBF should be ascribed to the dissolution and bioactivity behavior of those two phases.

Fig. 6 shows the SEM morphologies of samples sintered at various temperatures after soaking in SBF for 7 days. Apatite formation is more obvious on the samples surfaces sintered at 700, 900 and 1000 °C, as shown in Fig. 6(a)–(c). However, appreciable differences can also be observed. After soaking for 7 days, the surface of sample sintered at 700 °C was fully covered by one apatite layer, and this layer was composed of numerous spherical particles. For the sample sintered at 900 °C, the newly formed apatite layer was compact. However, for the sample sintered at 1000 °C, the sample surface was not fully covered and aggregation was observed in some zones. Different from that of above three samples, the surface of sample sintered at 1200 °C was only partially covered by a little small spherical particles. Furthermore, on the sample surface numerous pores were observed after soaking in SBF, which may be caused by sintering process or dissolution of crystallization phase in soaking.

4. Discussion

The XRD results of samples sintered at various temperatures (Fig. 2) show that the amorphous glasses were obtained at 700 °C, which was agreed with the results of TG/DTA. It is indicated that the previous heat treatment at 700 °C is enough for complete elimination of the nitrates used in the experiment. However, the double peaks at 570 and 603 cm^{-1} relating to the presence of crystalline phosphate in the sample (Fig. 3) seem to show a contradiction with the results obtained by XRD. The contradiction can be explained by the fact that the technology of FTIR probes short-range structural order, whereas XRD reveals long-range order in the glass structure. Moreover, taking into account the high bioactivity of the glasses composition combined with the powder form, tiny crystalline phase may be formed under atmospheric conditions. When the samples were sintered at 900 and 1000 °C, crystallization occurred and a glass-ceramics with pseudowollastonite and wollastonite phases were formed. And it is worth noting that the pseudowollastonite phase was formed at lower temperature than that obtained using the quenching technique method [27]. Probably, it should be due to the higher reactivity of the powders synthesized by sol–gel method. In addition, as we known, pseudowollastonite phase is one stable phase at high temperature, and the transformation from wollastonite to pseudowollastonite phase should take place with the temperature increasing. However, with the increase of sintering temperature, it was found that the pseudowollastonite phase gradually decreased accompanying by the increase of wollastonite. Especially, in the case of samples sintered at 1200 °C, it was observed that wollastonite replaced pseudowollastonite as the primary phase. The reason should be attributed to the crystallization of tricalcium phosphate, the existence of tricalcium phosphate seemed to stabilize the wollastonite phase even at high temperatures [28].

The surface modifications of samples sintered at various temperatures after soaking in SBF are comprehensively detected by XRD, FTIR and SEM. On the basis of these results, we conclude that samples sintered at various temperatures all possess the bioactivity, however, the formation rate of apatite layer decreases with the temperature increase. The apatite formation on bioactive glasses was studied and the reactions occurred on material surface were proposed by Hench and coworkers [29]. It was proposed that a rapid cation exchange between Na^+ or Ca^{2+} of material and H^+ or H_3O^+ from the solution took place, which induced the formation of SiO_2-rich layer on glass surface, then Ca^{2+} and PO_4^{3-} in

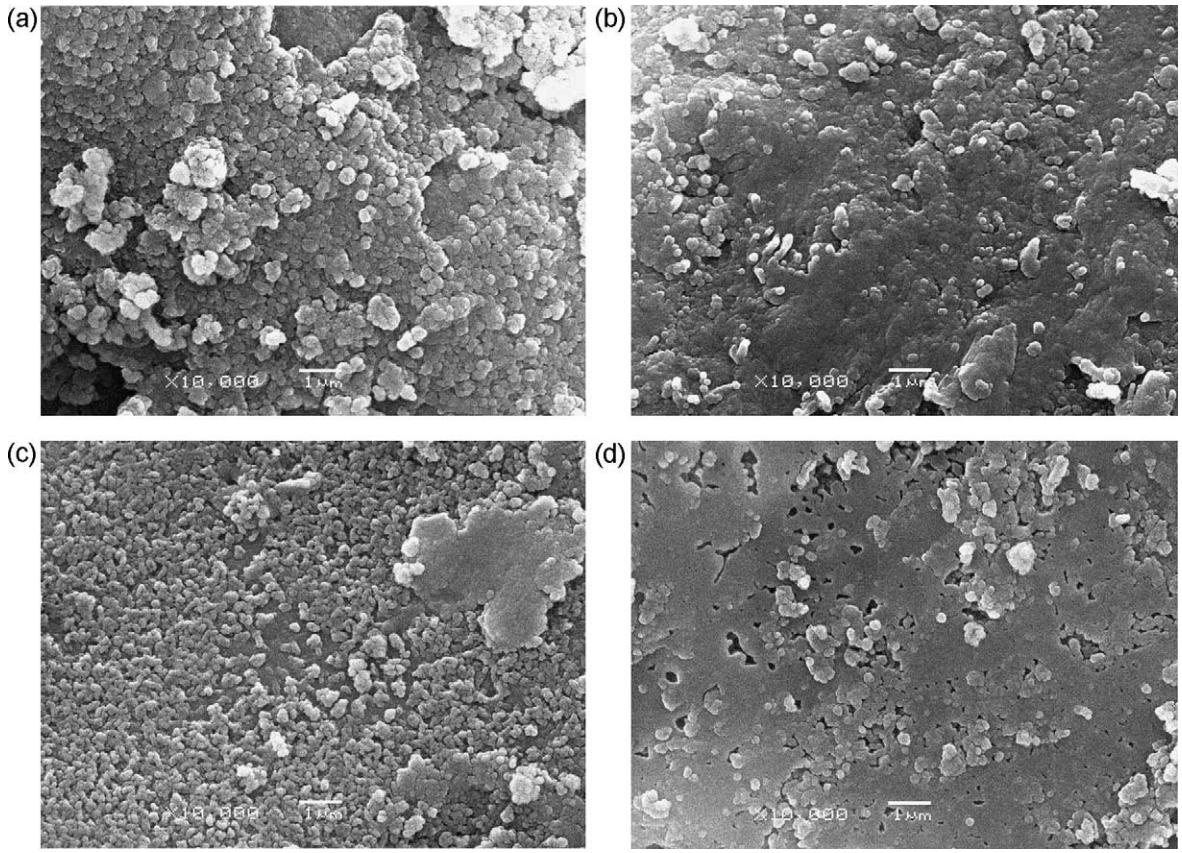

Fig. 6. SEM micrographs of the samples sintered at 700 °C (a), 900 °C (b), 1000 °C (c) and 1200 °C (d) after soaking in SBF for 7 days.

solution were migrated onto SiO_2-rich layer followed by nucleation and growth of apatite at the expense of the ions in the solution. When the gel was sintered at 700 °C which was lower than that necessary for the crystallization, the sample still kept the amorphous characteristic and the NBO bonds of Si–O–Ca was also observed (Fig. 3). Calcium oxide, as a network modifier, can insert into glass structure, induce the disruption of bridging oxygen bonds and lead the formation of NBO bonds. Some researches have demonstrated that the ion exchange is favored by the presence of Si–O–NBO bonds in the glass network and a minimum concentration is required in order to have an efficient ion exchange, dissolution of the silica and formation of a SiO_2-rich layer on the surface [30,31]. On the other hand, when the samples were sintered at higher temperatures, the crystallization occurred and glass-ceramics were obtained. Although the formation of the apatite on glass-ceramics was confirmed by the XRD, FTIR and SEM, the surface behavior of these samples was quite different. After 7 days of soaking in SBF, the sample sintered at 700 °C was fully covered by tiny spherical apatite particles. When the crystallization occurred in samples, crystal phases appeared and strong ionic bonds were formed between calcium cation and other functional groups. The higher the sintering temperature, the greater the degree of sample crystallization, and crystallization restricted the process of ions exchange and therefore delayed the formation of apatite layer, which could be observed in Fig. 6. Especially for the sample sintered at 1200 °C, after 7 days of soaking the glass-ceramics surface did not fully covered with apatite layer, although wollastonite phase has been reported to show bioactivity [32,33]. Moreover, crystal structure may also affect the bioactivity property of the glass-ceramics. Pseudowollastonite and wollastonite both belong to triclinic, but the crystal structures are different. Pseudowollastonite and wollastonite possess rings and chain structure, respectively. The difference of crystal structure may result in the difference of the stability, which may affect the degradation rate of the samples. Therefore, further studies are required to determine the relationship between the crystal structure and the degradation property of the glass-ceramics.

5. Conclusion

Glass and glass-ceramics have been obtained as a result of heat treatment of sol–gel derived 58S bioglass. It was found that the 58S bioglass crystallized at the temperature range of 890–929 °C. And with the increase of sintering temperature, the crystalline wollastonite phase replaced pseudowollastonite as the primary phase. The results of in vitro assays indicated that the crystallization decreased the bioactivity of the 58S bioglass. A dense apatite layer composed of numerous spherical particles was formed on the highly bioactive amorphous 58S bioglass, whereas incomplete or porous apatite layer was formed on the bioglass subjected to crystallization.

Acknowledgements

This work was financially supported by the Department of Science and Technology of Shandong Province (Grant No. 2006GG3203006) and Department of Science and Technology of Jinan, Shandong Province (Grant No. 051070), P. R. China.

References

[1] L.L. Hench, R.J. Splinter, W.C. Allen, T.K. Greenlee, Bonding mechanism at interface of ceramic prosthetic materials, J. Biomed. Mater. Res. 2 (1972) 117–141.
[2] W. Vogel, W. Holand, Development, structure, properties and application of glass-ceramics for medicine, J. Non-Cryst. Solids 123 (1990) 349–353.
[3] T. Turunen, J. Peltola, R.P. Happonen, A. Yli-Urpo, Effect of bioactive glass granules and polytetrafluoroethylene membrane on repair of cortical bone defect, J. Mater. Sci.-Mater. Med. 11 (1995) 639–641.
[4] L.L. Hench, Bioceramics, J. Am. Ceram. Soc. 81 (1998) 1705–1728.
[5] A. Balamurugan, G. Sockalingum, J. Michel, J. Fauré, V. Banchet, L. Wortham, S. Bouthors, D. Laurent-Maquin, G. Balossier, Synthesis and characterisation of sol gel derived bioactive glass for biomedical applications, Mater. Lett. 60 (2006) 3752–3757.
[6] L.L. Hench, Bioceramics: from concept to clinics, J. Am. Ceram. Soc. 74 (1991) 1487–1510.
[7] K. Franks, I. Abrahams, G. Georgious, J.C. Knowles, Investigation of thermal parameters and crystallisation in a ternary $CaO–Na_2O–P_2O_5$-based glass system, Biomaterials 22 (2001) 497–501.
[8] J.D. Santos, P.L. Silva, J.C. Knowles, S. Talal, F.J. Monteriro, Reinforcement of hydroxyapatite by adding P_2O_5–CaO glasses with Na_2O, K_2O and MgO, J. Mater. Sci.-Mater. Med. 7 (1996) 187–189.
[9] M. Brink, T. Turunen, R.P. Haponen, A. Yli-Urpo, Compositional dependence of bioactivity of glasses in the system $Na_2O–K_2O–MgO–CaO–B_2O_3–P_2O_5–SiO_2$, J. Biomed. Mater. Res. Part A 37 (1997) 114–121.
[10] J.P. Zhong, D.C. Greenspan, Processing and properties of sol–gel bioactive glasses, J. Biomed. Mater. Res. Part B 53 (2000) 694–701.
[11] A. Martínez, I. Izquierdo-Barba, M. Vallet-Regí, Bioactivity of a $CaO–SiO_2$ binary glasses system, Chem. Mater. 12 (2000) 3080–3088.
[12] T. Kokubo, M. Shigematsu, Y. Nagashima, M. Tashiro, T. Yamamuro, S. Higashi, Apatite- and wollastonite-containing glass-ceramics for prosthetic application, Bull. Inst. Chem. Res. Kyoto Univ. 60 (1982) 260–268.
[13] K. Ono, T. Yamamuro, T. Nakamura, T. Kokubo, Quantitative study on osteoconduction of apatite–wollastonite containing glass-ceramic granules, hydroxyapatite granules and alumina granules, Biomaterials 11 (1990) 265–271.
[14] T. Kitsugi, T. Yamamuro, T. Nakamura, T. Kokubo, Bonding behavior of $MgO–CaO–SiO_2–P_2O_5–CaF_2$ glass (mother glass of AW-glass-ceramics), J. Biomed. Mater. Res. 23 (1989) 631–648.
[15] T. Kitsugi, T. Yamamuro, T. Nakamura, T. Kokubo, The bonding of glass ceramics to bone, Int. Orthoped. 13 (1989) 199–206.
[16] T. Kokubo, H. Kushitani, S. Sakka, T. Kitsugi, T. Yamamuro, Solutions able to reproduce in vivo surface-structure changes in bioactive glass-ceramic $A\text{-}W^3$, J. Biomed. Mater. Res. 24 (1990) 721–734.
[17] W. Höland, W. Vogel, K. Naumann, J. Gummel, Interface reactions between machinable bioactive glass-ceramics and bone, J. Biomed. Mater. Res. 19 (1985) 303–312.
[18] S. Radin, P. Ducheyne, B. Rothman, A. Conti1, The effect of in vitro modeling conditions on the surface reactions of bioactive glass, J. Biomed. Mater. Res. Part A 37 (1997) 363–375.
[19] J.L. Arias, F.J. García-Sanz, M.B. Mayor, S. Chiussi, J. Pou, B. León, M. Pérez-Amor, Physicochemical properties of calcium phosphate coatings produced by pulsed laser deposition at different water vapor pressures, Biomaterials 19 (1998) 883–888.
[20] P. Gonzáalez, J. Serra, S. Liste, S. Chiussi, B. León, M. Pérez-Amor, Ageing of pulsed-laser-deposited bioactive glass films, Vacuum 67 (2002) 647–651.
[21] S.Y. Ni, J. Chang, L. Chou, A novel bioactive porous $CaSiO_3$ scaffold for bone tissue engineering, J. Biomed. Mater. Res. Part A 76 (2006) 196–205.
[22] A. Binnaz Yoruç Hazar, Preparation and in vitro bioactivity of $CaSiO_3$ powders, Ceram. Int. 33 (2007) 687–692.
[23] C. Ohtsuki, T. Kokubo, T. Yamamuro, Mechanism of apatite formation on $CaO–SiO_2–P_2O_5$ glasses in a simulated body fluid, J. Non-cryst. Solids 143 (1992) 84–92.
[24] P. Li, C. Ohtsuki, T. Kokubo, K. Nakanishi, N. Soga, T. Nakamura, T. Yamamuro, Process of formation of bone-like apatite layer on silica gel, J. Mater. Sci.-Mater. Med. 4 (1993) 127–131.
[25] P.N. DeAza, J.M. Fernández-Pradas, P. Serra, In vitro bioactivity of laser ablation pseudowollastonite coating, Biomaterials 25 (2004) 1983–1990.
[26] Y. Iimori, Y. Kameshima, K. Okada, S. Hayashi, Comparative study of apatite formation on $CaSiO_3$ ceramics in simulated body fluids with different carbonate concentrations, J. Mater. Sci.-Mater. Med. 16 (2005) 73–79.
[27] B. Philips, A. Muan, Phase equilibria in the system CaO–iron oxide–SiO_2 in air, J. Am. Ceram. Soc. 42 (1959) 413–423.
[28] J. Román, S. Padilla, M. Vallet-Regí, Sol–gel glasses as precursors of bioactive glass ceramics, Chem. Mater. 15 (2003) 798–806.
[29] O. Peitl, E.D. Zanotto, L.L. Hench, Highly bioactive $P_2O_5–Na_2O–CaO–SiO_2$ glass-ceramics, J. Non-Cryst. Solids 292 (2001) 115–126.
[30] J. Serra, P. Gonzalez, S. Liste, S. Chiussi, Influence of the non-bridging oxygen groups on the bioactivity of silicate glasses, J. Mater. Sci.-Mater. Med. 13 (2002) 1221–2122.
[31] Y.F. Zhao, M.D. Song, C.Z. Chen, J. Liu, The role of the pressure in pulsed laser deposition of bioactive glass films, J. Non-cryst. Solids 354 (2008) 4000–4004.
[32] L.H. Long, L.D. Chen, J. Chang, Low temperature fabrication and characterizations of β-$CaSiO_3$ ceramics, Ceram. Int. 32 (2006) 457–460.
[33] H.H. Rodriguez, G. Vargas, D.A. Cortés, Electrophoretic deposition of bioactive wollastonite and porcelain-wollastonite coatings on 316L stainless steel, Ceram. Int. 34 (2008) 1303–1307.